Flux rope formation and evolution

P. Romano[(1)] , S.L. Guglielmino[(2)], M. Falco[(1)], F. Zuccarello[(2)]

[(1)]INAF – Catania Astrophysical Observatory, Catania, Italy;
[(2)]Dipartimento di Fisica e Astronomia “Ettore Majorana” – Università degli Studi di Catania, Catania, Italy

November 12th, 2019 Padova (Italy)

7th Metis Workshop 2019

On March 30, 2010, at 304 Angstrom from AIA onboard of SDO…

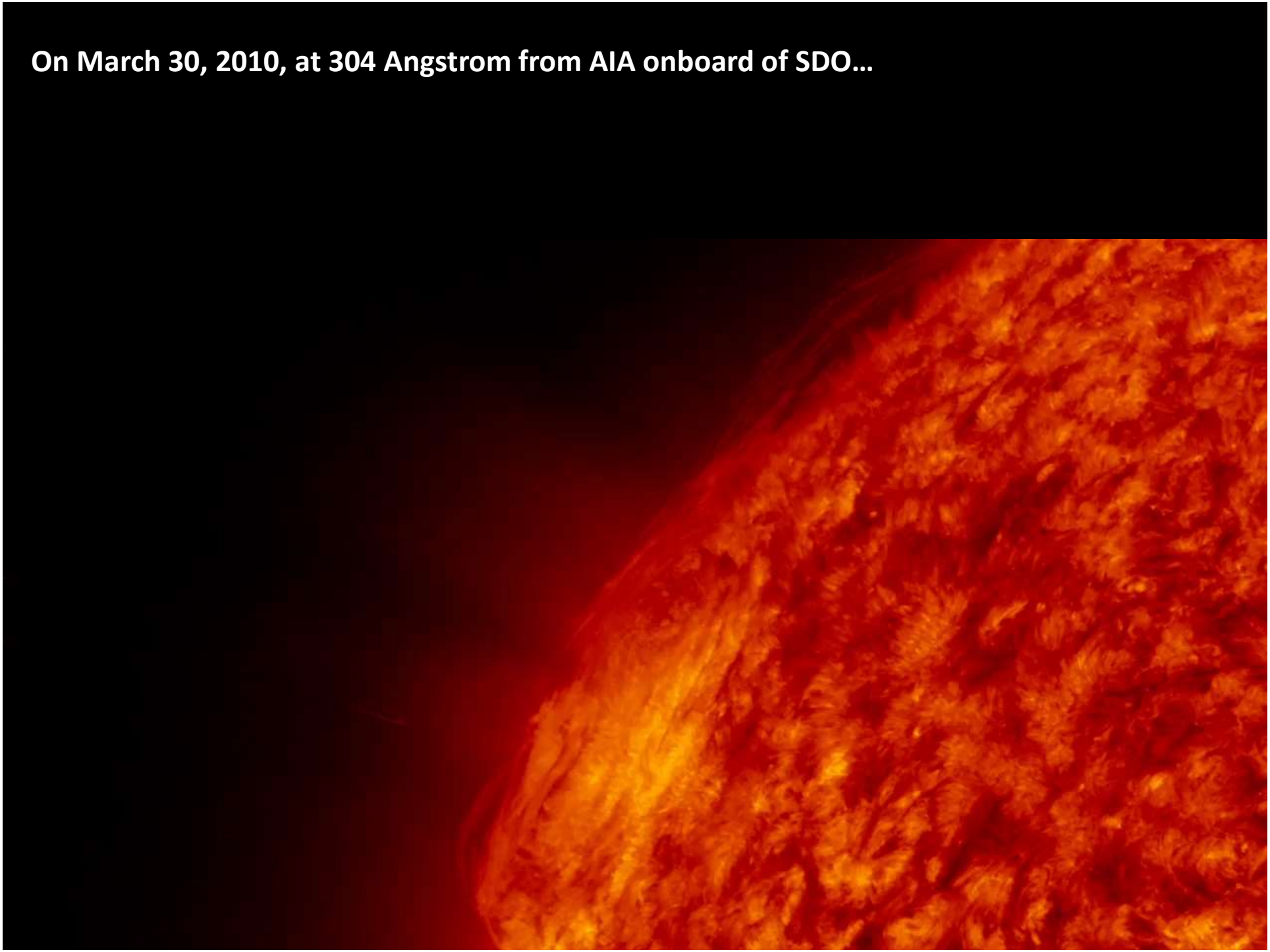

Sigmoids are other manifestation of magnetic field lines that collectively wrap around a central, axial field line

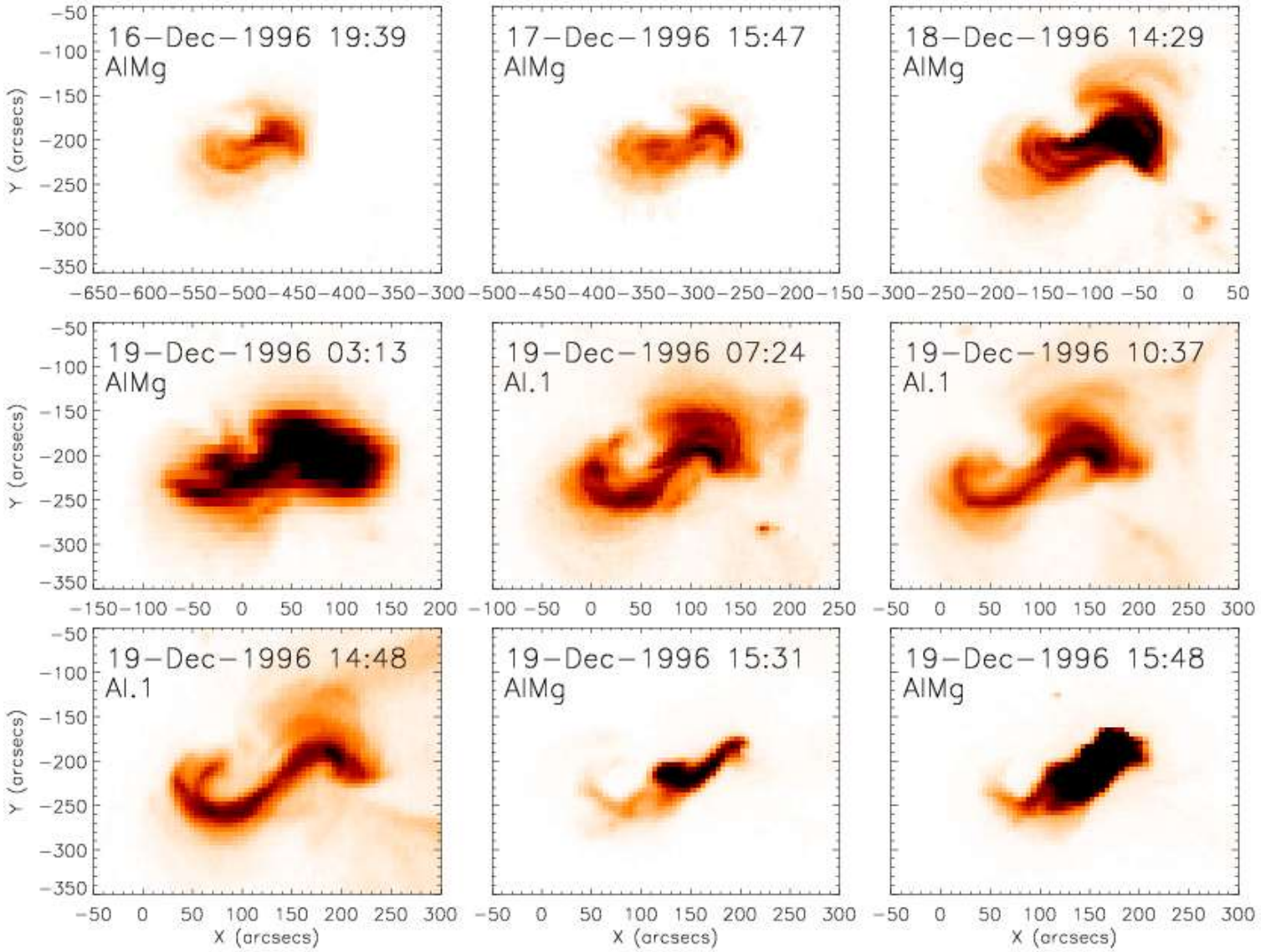

Green & Kliem (2009)

Flux ropes and magnetic helicity injection

CMEs are thought to be the primary agent through which the Sun gets rid of its excess helicity (Rust 1994; Low 1996; Zhang et al. 2005, 2006, 2012; Zhang and Flyer, 2008).

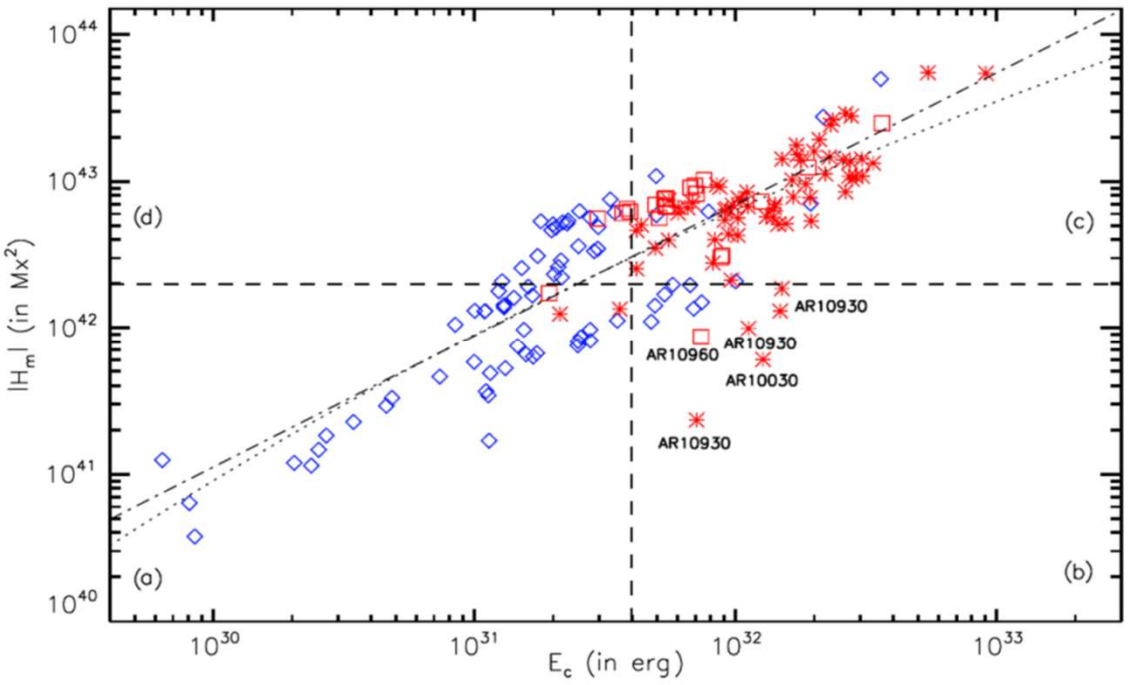

Tziotziou et al., 2012

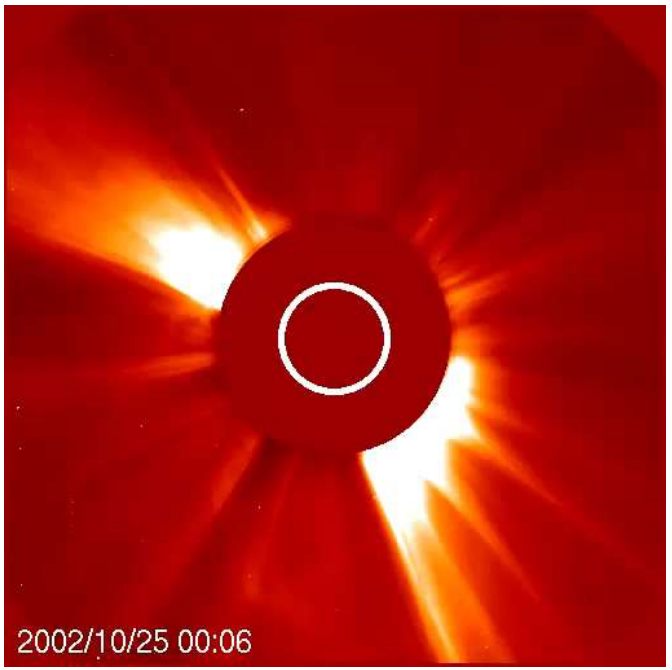

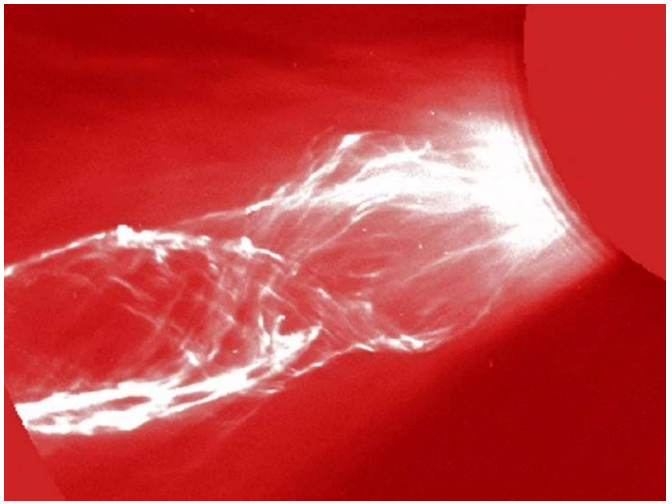

Magnetic topology at eruption onset & initial equilibrium

Arcade of loops

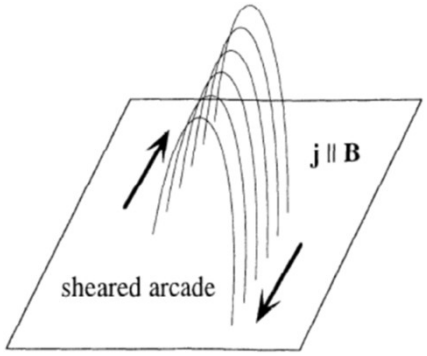

– arcade → FR (transition?)

Flux rope (FR)

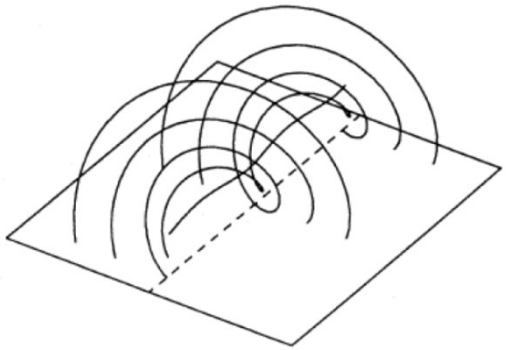

Onset, drive mechanism(s) & acceleration

Tether Cutting

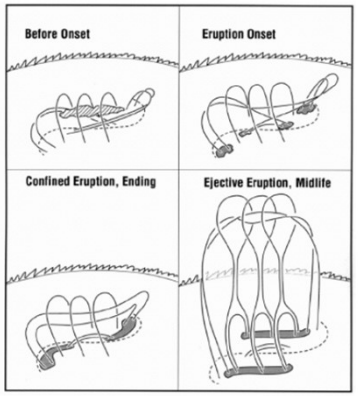

Magnetic Breakout

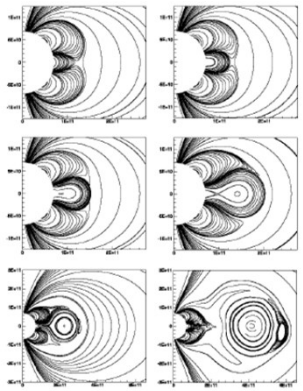

Flux Rope Catastrophe

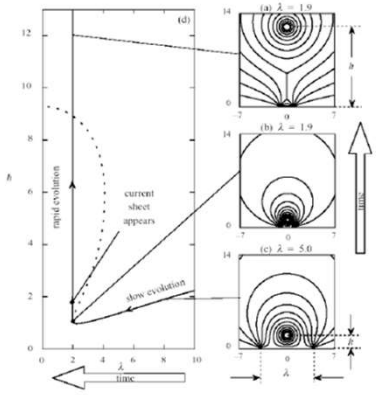

Flux Rope Instability (torus / kink)

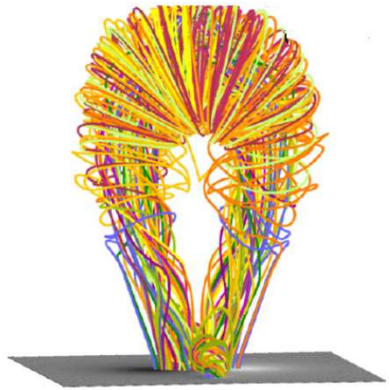

Filaments in their stable equilibrium prior to eruption are contained in fields of flux rope or arcade topology (?)

Torus instability

The torus instability model predicts that a magnetic flux rope of major radius R undergoes an eruption when its axis reaches a location where the **decay index**:

$$n = \frac{d(\ln B_{ex})}{d(\ln R)}$$

of the ambient field B_{ex} is larger than a critical value (n_{crit} = 1.5 for Kliem & Török , 2006)

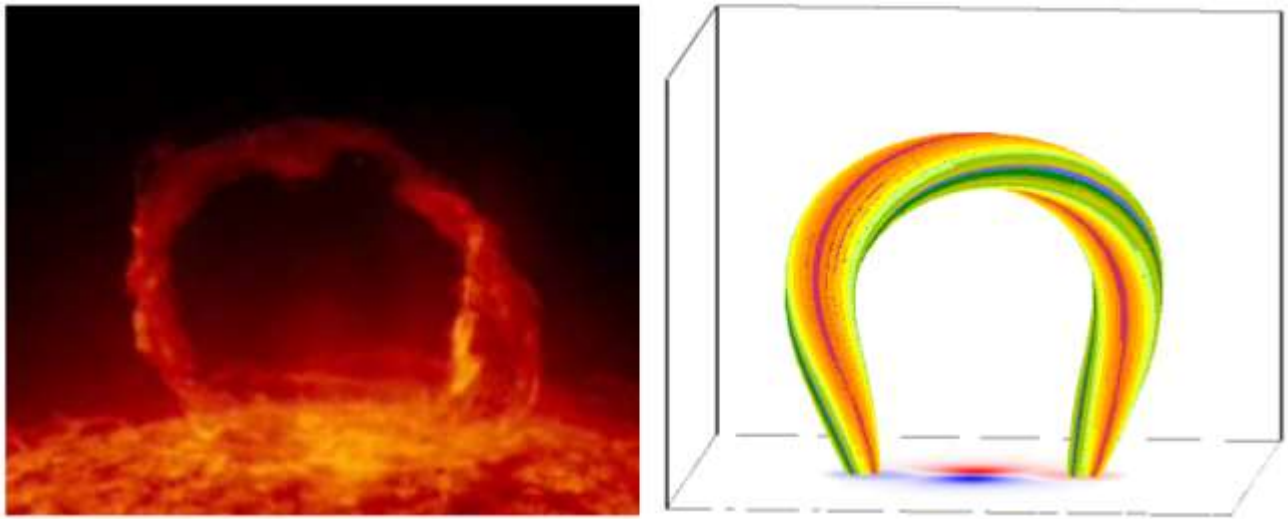

High twist, $\phi = 2\pi N > \phi cr = (2.5 \ldots 5)\pi$, additionally triggers the helical (m = 1) kink mode

(Fan & Gibson 2003; Török et al. 2004)

Homologous white light flares

SOL2017-09-06T09:10 (X2.2) & SOL2017-09-06T12:02 (X9.3)

304 Å 171 Å 131 Å

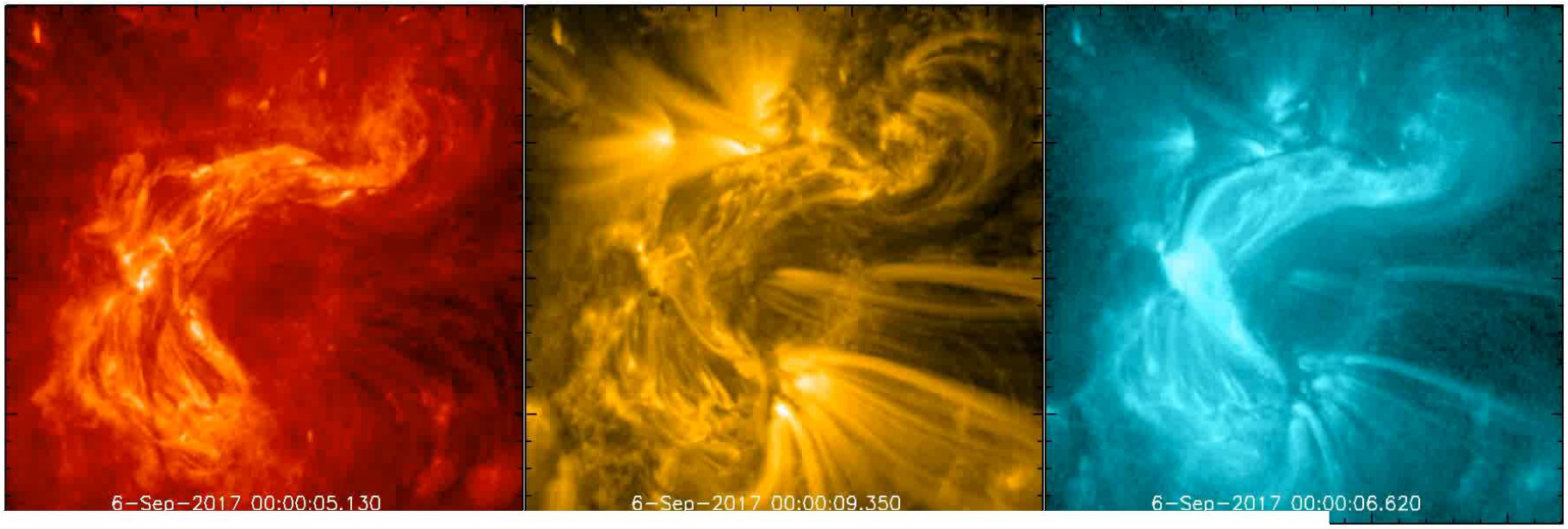

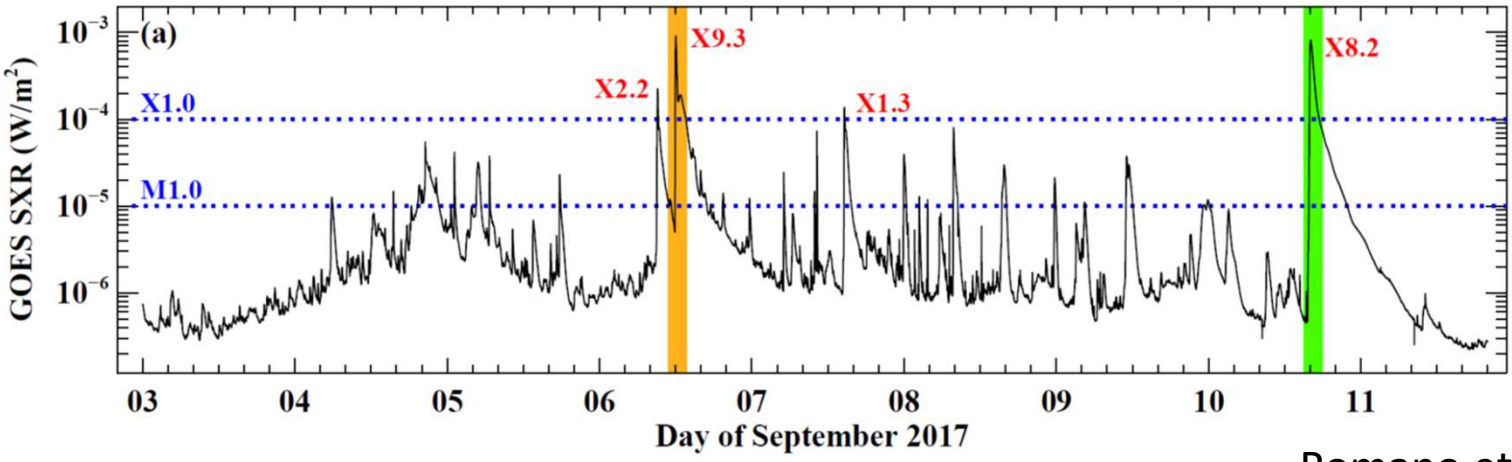

Romano et al. (2018, 2019)

Homologous flares

SOL2017-09-06T09:10 (X2.2) & SOL2017-09-06T12:02 (X9.3)

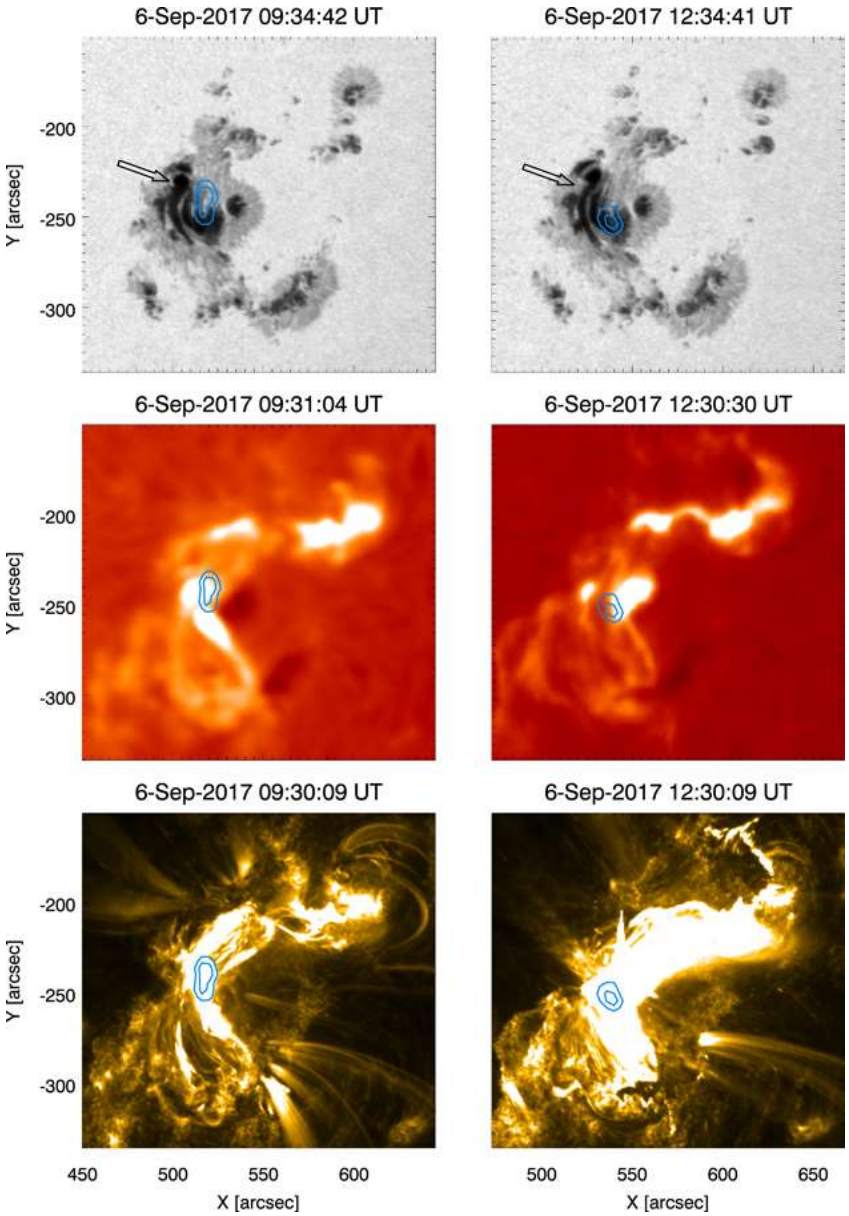

	Start	Peak	End
X2.2	8:57 UT	9:10 UT	9:17 UT
X9.4	11:53 UT	12:02 UT	12:10 UT

We can identify three regions where the detector reached its saturation level:

- one above the delta spot,
- one at the northern edge of the penumbra,
- one above the smaller negative sunspots on the northwest side relative to the delta spot.

HXR sources (12-25 keV) for both WLFs do not seem to be located above the elongated negative umbra, but rather at its western side, i.e., in the center of the delta spot.

Romano et al. (2018)

Homologous white light flares

SOL2017-09-06T09:10 (X2.2) & SOL2017-09-06T12:02 (X9.3)

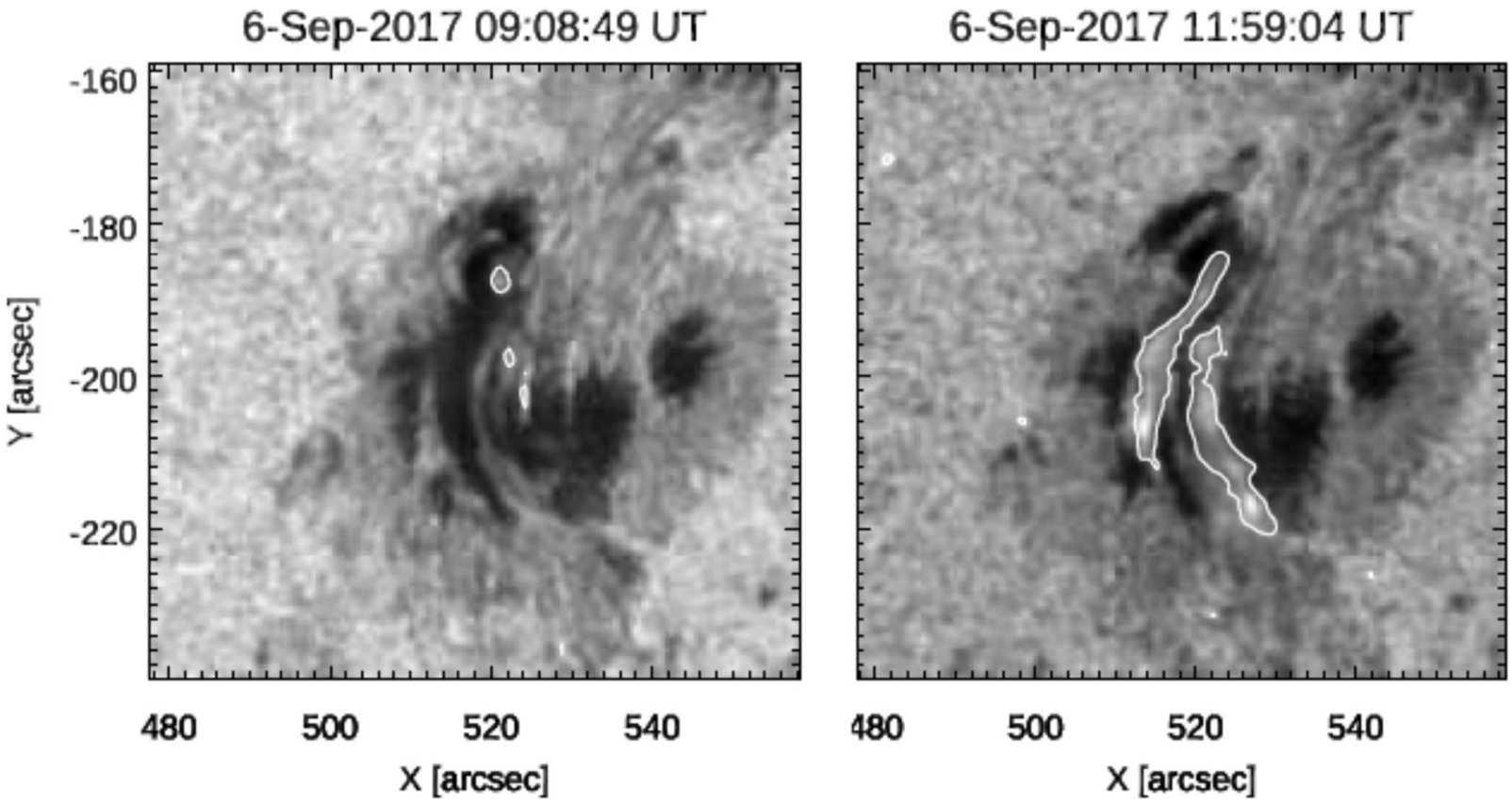

The area of the kernels reached a total maximum extension of about 2.4×10^6 km^2 and 9.2×10^7 km^2 during the X2.2 and X9.3 flares, respectively.

Romano et al. (2018)

3D null points

00:00 UT | 08:48 UT | 11:48 UT

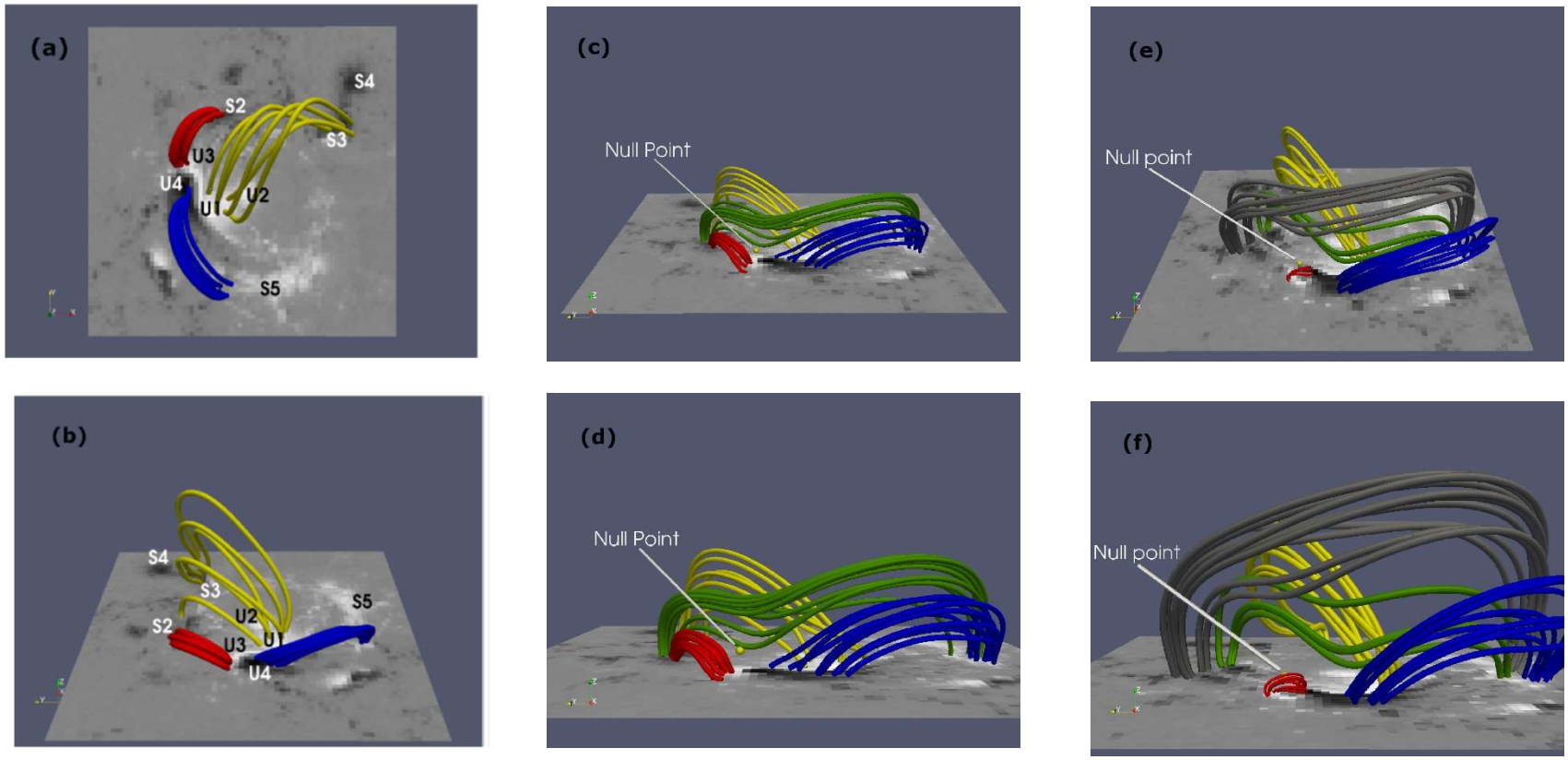

He, Wang, and Yan (2011)

- We identified two related 3D null points located at **low heights** above the photosphere (**5000** km and **3000** km).

- Their formation at such low altitudes may plausibly be ascribed to the peculiar photospheric horizontal motions

Romano et al. (2019)

Torus instability

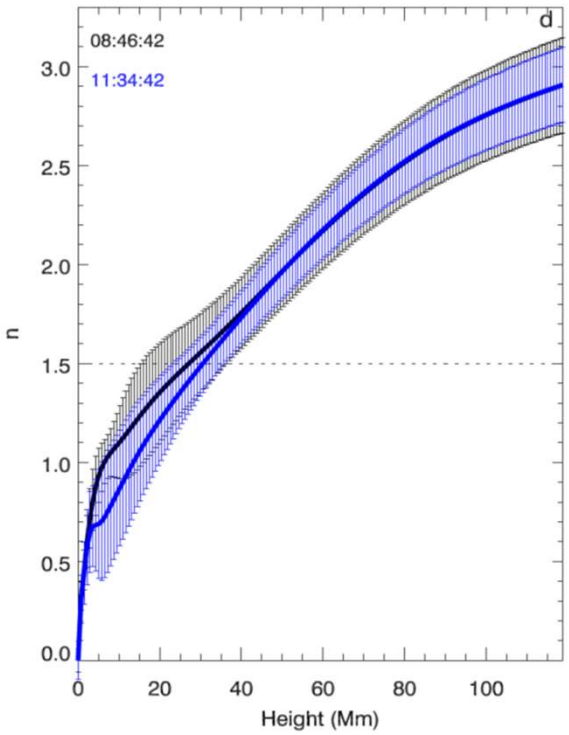

NLFF extrapolation (Wiegelmann 2004; Wiegelmann et al. 2012)

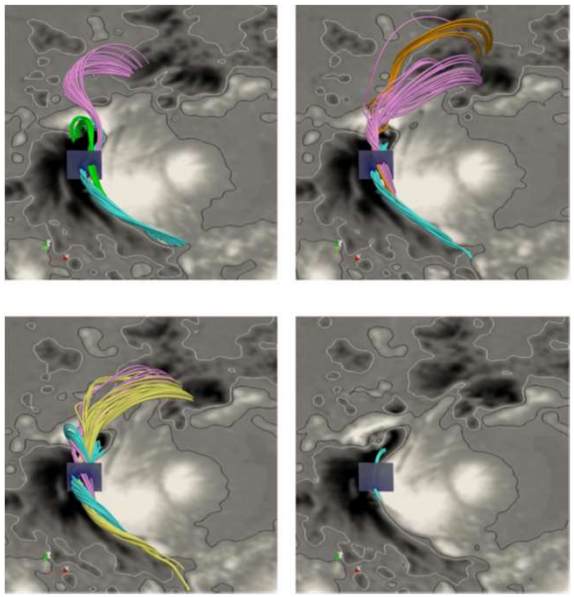

Jiang et al. (2018)

Liu et al. (2018)

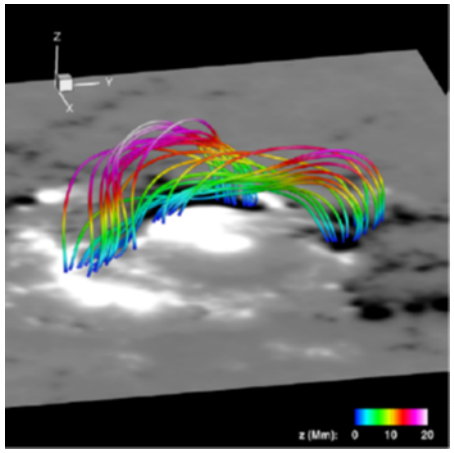

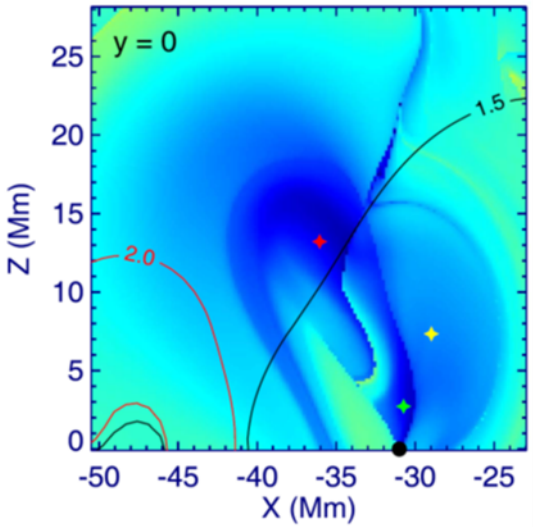

The FR was already in an unstable regime, suggesting that the eruption is more likely a result of TI rather than KI.

Jiang et al. (2018)

Double decker flux rope

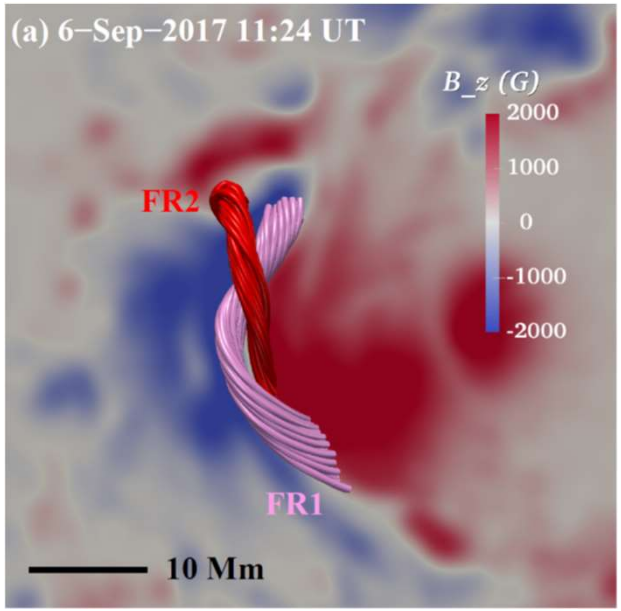

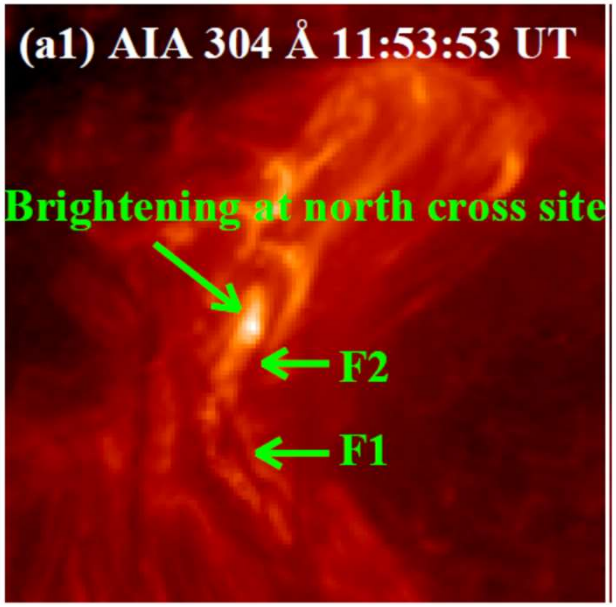

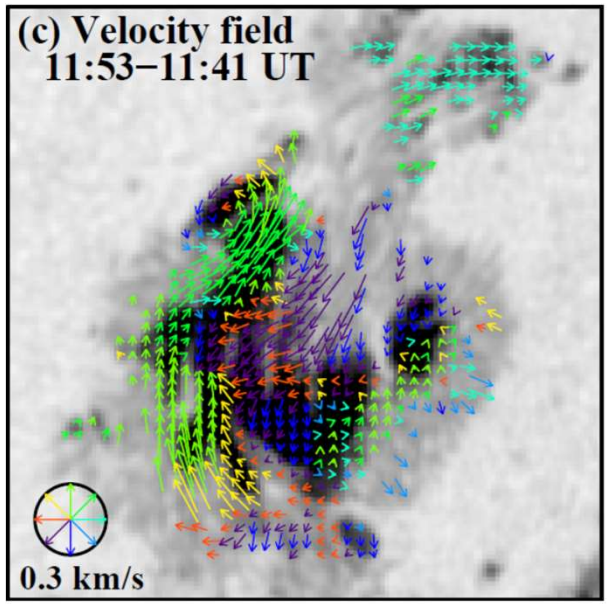

NLFFF extrapolation (Wiegelmann 2004; Wiegelmann et al. 2012)

$T_w \leq -1.0$ (flux ropes) $T_w = \frac{1}{4\pi}\int \frac{\nabla \times \boldsymbol{B} \cdot \boldsymbol{B}}{|\boldsymbol{B}|^2} dl,$

The double decker flux rope configuration seems to laying above the semicircular PIL.

The **strong shear motion and rotation**.

Kink instability ??

Hou et al. (2018)

The role of helicity injection and surrounding magnetic field

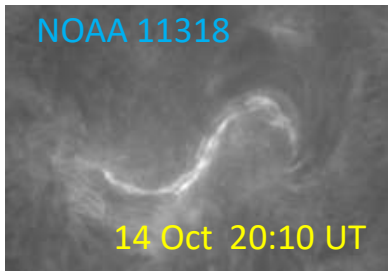

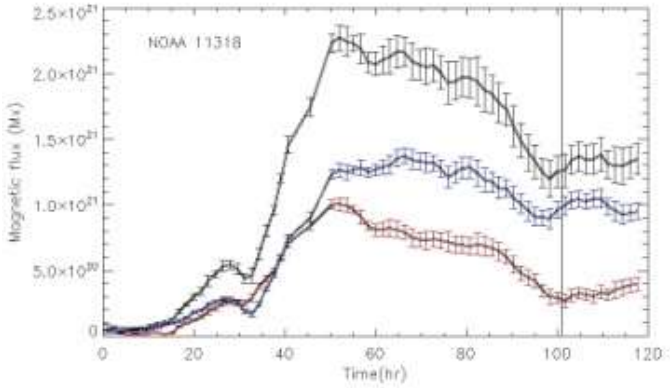

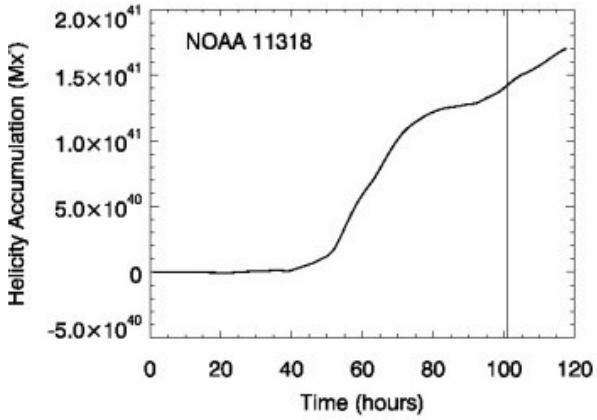

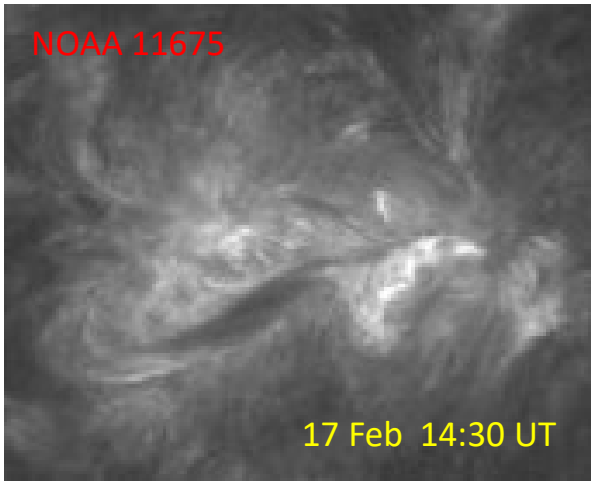

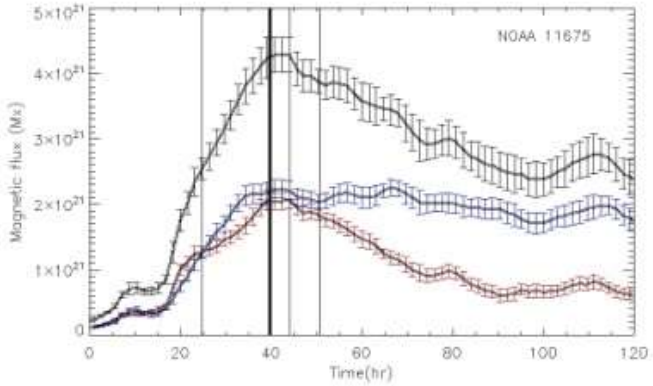

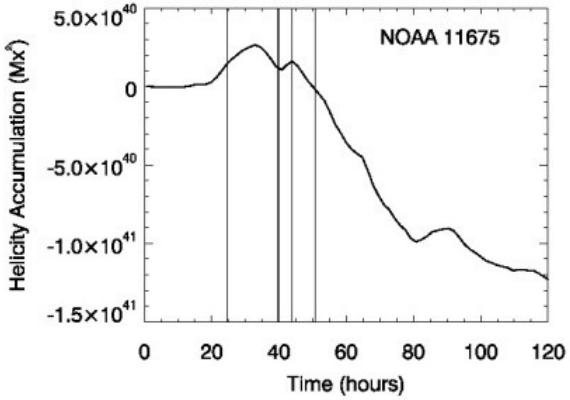

The role of helicity injection and surrounding magnetic field

NOAA 11318

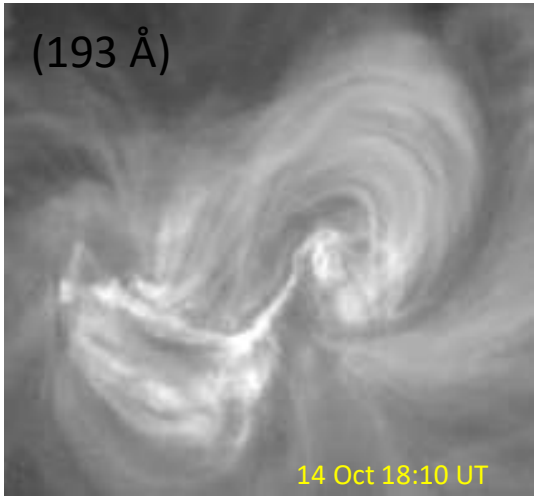

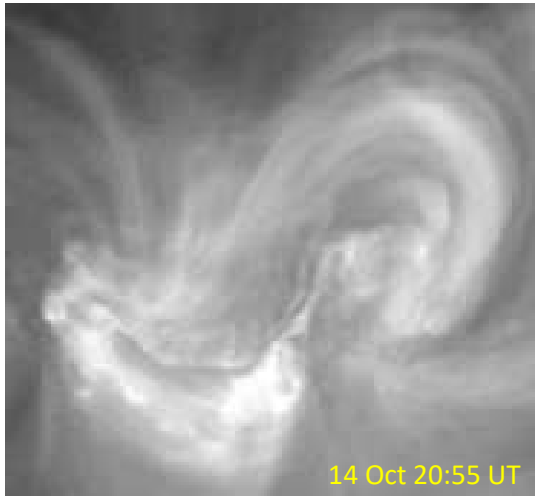

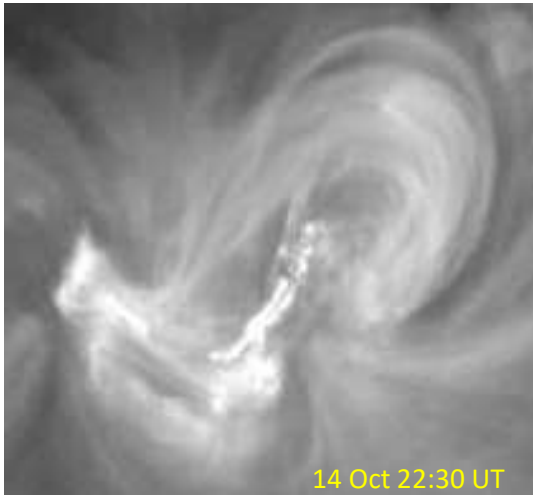

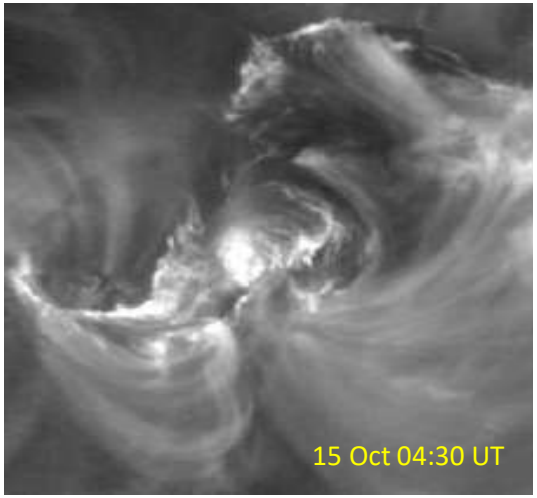

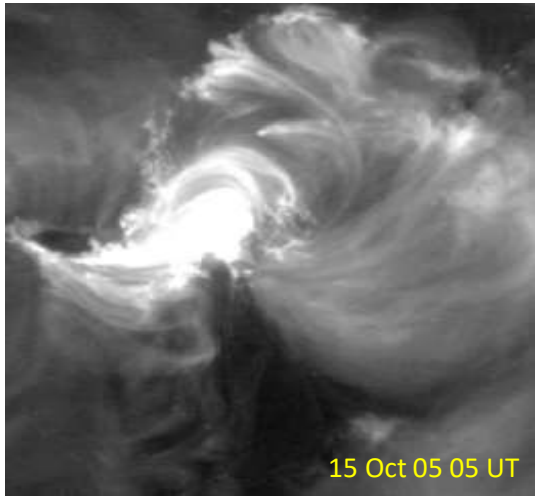

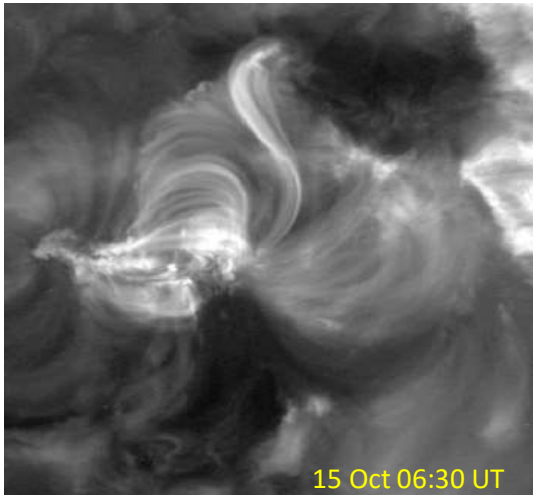

The role of helicity injection and surrounding magnetic field

NOAA 11675

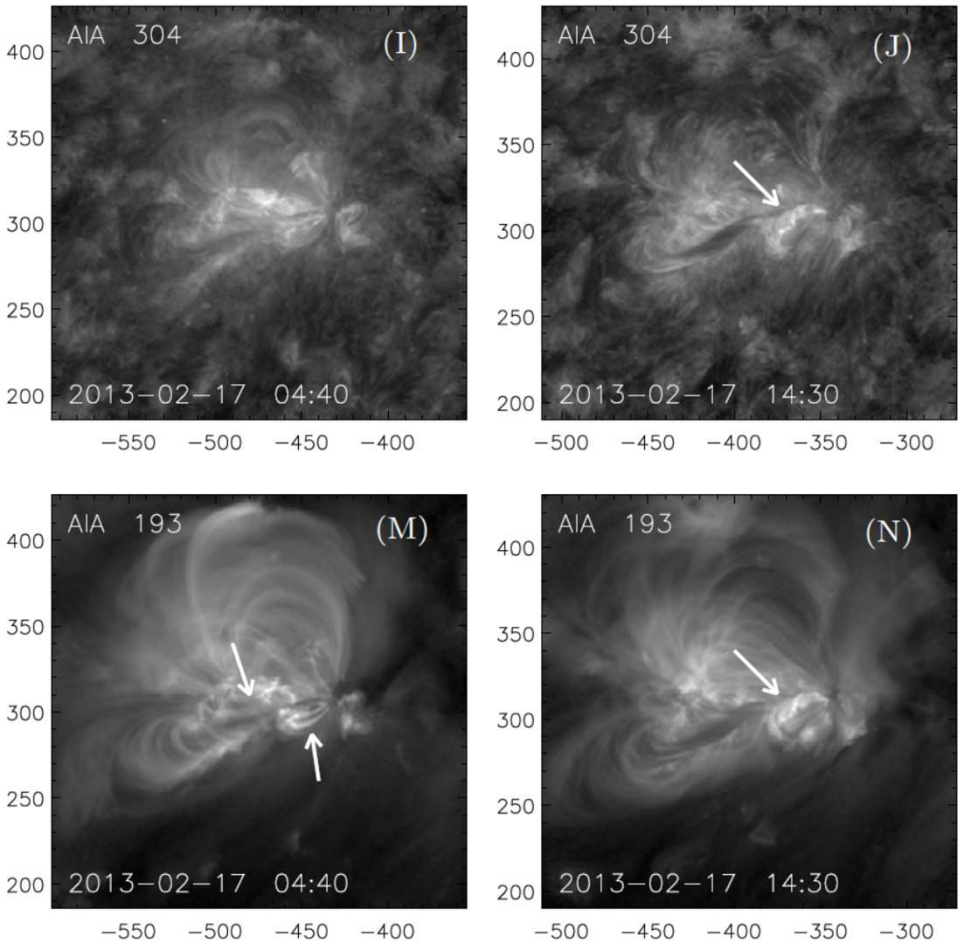

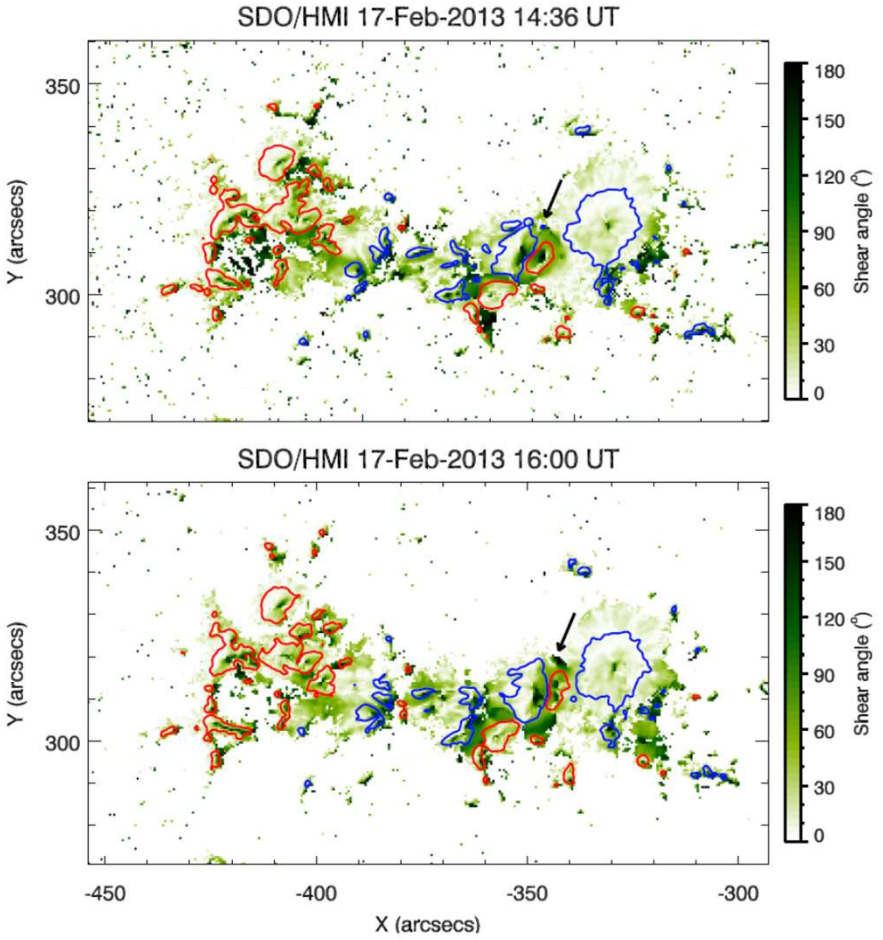

Gosain & Venkatakrishnan, 2010

$$\theta = \arccos \frac{\mathbf{B}_{\mathbf{h}}^{\mathrm{obs}} \cdot \mathbf{B}_{\mathbf{h}}^{\mathrm{pot}}}{\left|B_h^{\mathrm{obs}}\right|\left|B_h^{\mathrm{pot}}\right|},$$

The role of helicity injection and surrounding magnetic field

NOAA 11318

Day	Time (UT)	*GOES* Class
2011 Oct 15	04:19	**C2.3**

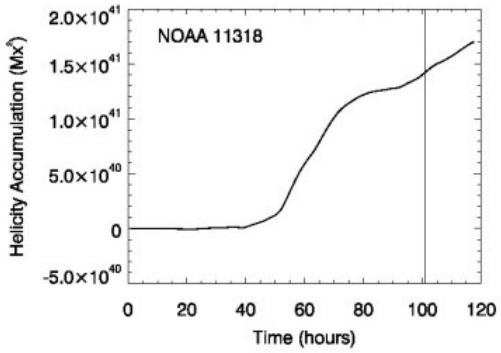

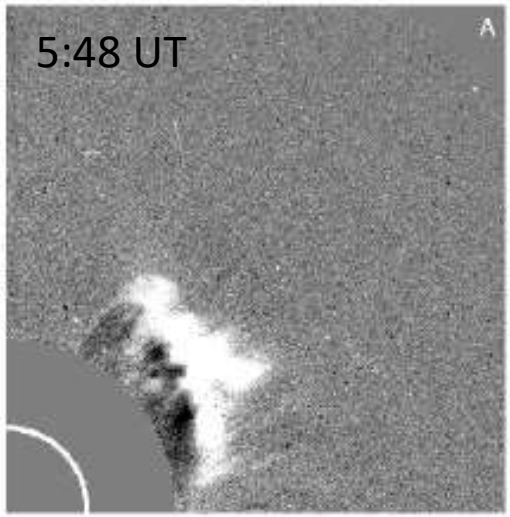

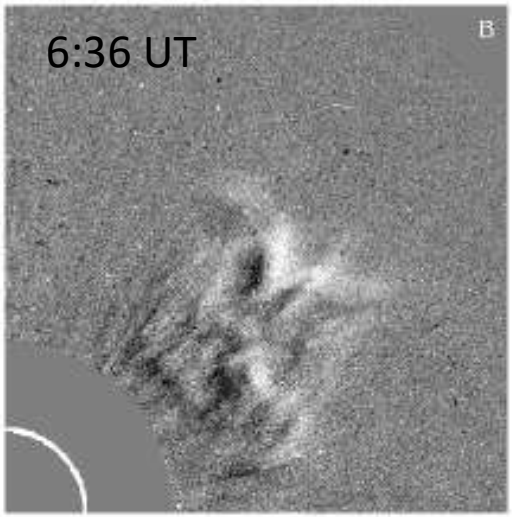

NOAA 11675

Day	Time (UT)	*GOES* Class
2013 Feb 17	00:36	C1.0
2013 Feb 17	15:40	C2.5
2013 Feb 17	15:50	**M1.9**
2013 Feb 17	20:00	C1.0
2013 Feb 18	02:41	C1.0

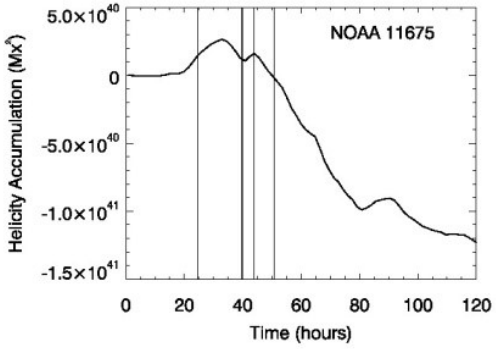

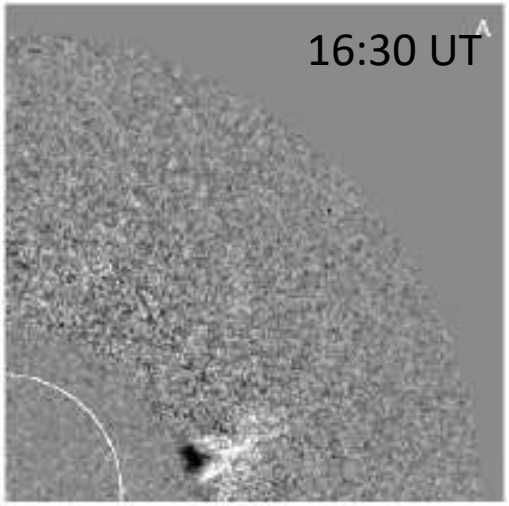

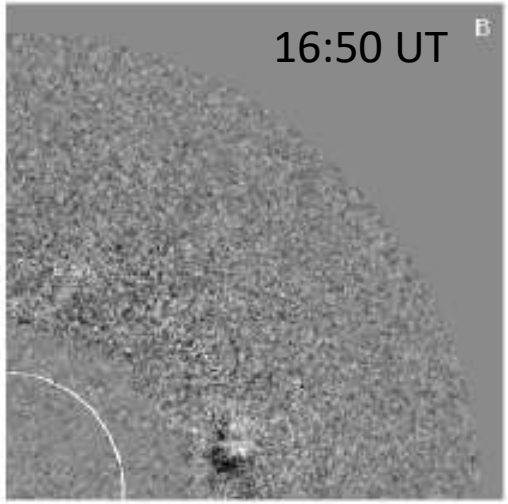

New opportunities…

The advantages of coordinated observations by the remote sensing instruments aboard Solar Orbiter and the new generation ground based telescopes:

- Coupling of high resolution and context observations
- Coupling between inner and outer layers of solar atmosphere

PHI

SPICE

EUI

METIS

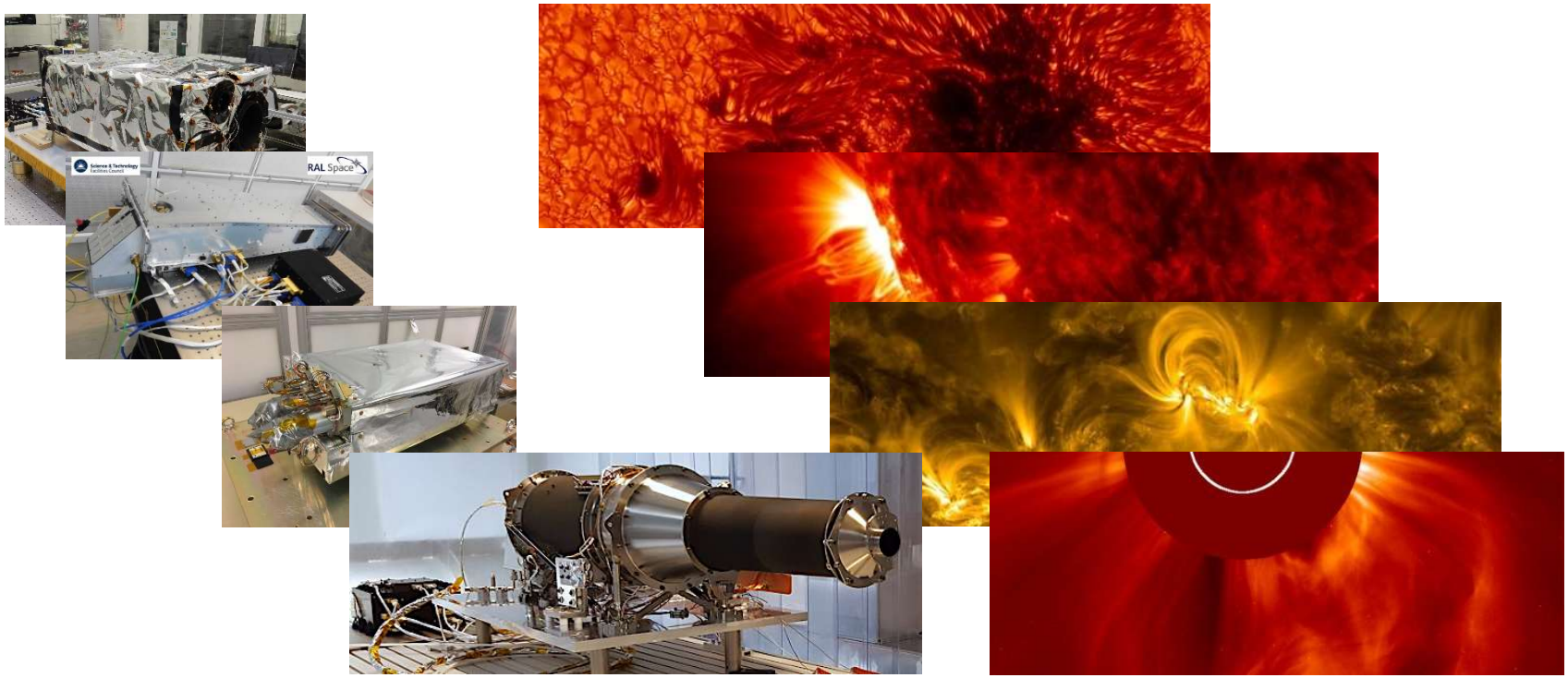

The stereoscopic polarimetry (besides stereoscopic imaging of the photosphere) ...

A reduced solar apparent rotation when following solar features …

In the later phase of the mission when the spacecraft will leave the ecliptic from a heliographic latitude of up to 33° …

Solar Orbiter

Identity of plasma in visible parts of a proto-CME on-disk and connect (via compositional correlation) to higher altitudes and in situ measurements.

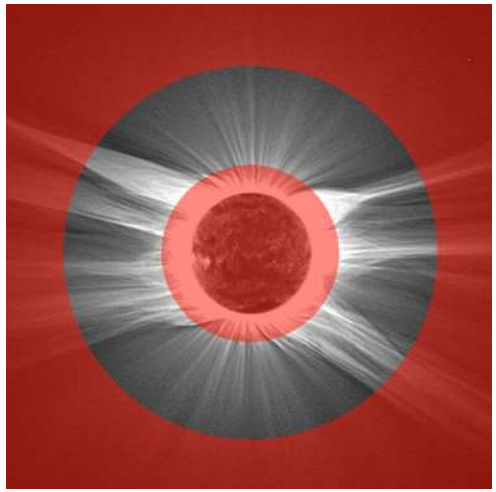

Magnetic topology at eruption onset

Initial equilibrium

Drive mechanism

CME evolution through the corona and inner heliosphere

- More precise measurements of the FR properties in the inner and outer corona (R, N, …)

- NLFFEs

- Decay Index

- Horizontal and vertical velocities at photospheric level

- Magnetic helicity injection

Conclusions

FR formation

Do FRs rise through the convection zone or are they formed in situ by an arcade-to-rope topology transformation?

FR geometry (torus instability?)

Reducing foreshortening effects and using spectroscopic observations, is it possible to verify FR models for eruption onset?

Role of non-ideal MHD

Does it trigger/drive the eruption?

Role of the overlying magnetic field

Configuration of FR and surrounding magnetic field (opposite sign of magnetic helicity? Antiparallel configuration?)

Magnetic helicity budget

Stereoscopic measurements of the photospheric velocities, overcaming of the 180° ambiguity, NLFFEs, connectivities…